Available online at www.sciencedirect.com
ScienceDirect
Journal of Nuclear Materials 357 (2006) 58–68
journal of nuclear materials
www.elsevier.com/locate/jnucmat

Fuel – cladding chemical interaction in MOX fuel rods irradiated to high burnup in an advanced thermal reactor

Kosuke Tanaka [a,*], Koji Maeda [a], Shinji Sasaki [a], Yoshihisa Ikusawa [b], Tomoyuki Abe [b]

[a] *O-arai Research and Development Center, Japan Atomic Energy Agency, 4002 Narita-cho, Oarai-machi, Higashi-ibaraki-gun, Ibaraki-ken 311 1393, Japan*

[b] *Tokai Research and Development Center, Japan Atomic Energy Agency 4-33 Muramatsu, Tokai-mura, Naka-gun, Ibaraki-ken 311 1194, Japan*

Received 11 August 2005; accepted 17 May 2006

Abstract

The performance of MOX fuel irradiated in the advanced thermal reactor, FUGEN, to a burnup of 47.5 GWd/t, was investigated by using a telescope, optical microscope, SEM and EPMA. Observations focused on elucidating the corrosion behavior of the cladding inner surface. A reaction layer was observed at burnups higher than about 35 GWd/t. The relationship between the thickness of the reaction layer and burnup was similar to that reported in the literature for conventional UO_2 fuel and other MOX fuels. The existence of a plutonium spot near the outer surface of the fuel pellet had no significant effect on the thickness of the reaction layer. A bonding layer was observed on the cladding inner surface. Its morphology and elemental distributions were not so different from those in BWR UO_2 fuel rods irradiated to high burnup, in which the fission gas release rate is high. In addition, the dependences of bonding layer formation on the burnup and linear heat rating were similar to results of UO_2 fuel rods. It was, thus, suggested that the bonding layer formation mechanism was similar in both UO_2 and MOX fuel rods.

PACS: 28.41.Bm

1. Introduction

The utilization of plutonium in nuclear reactors is the critical to save energy resources. Plutonium can be recycled most effectively in fast breeder reactors, but their high construction and operation costs have made it impossible to achieve commercial use. Then, thermal reactors which have a high conversion ratio of ^{238}U to ^{239}Pu have been considered as an alternative candidate. In Japan, the advanced thermal reactor (ATR) FUGEN, which was moderated by heavy water and cooled by light water, was developed and operated until March 2003. During its operational period, 772 MOX fuel assemblies were burned without failure [1,2].

* Corresponding author. Tel.: +81 29 267 4141; fax: +81 29 266 0016.
E-mail address: tanaka.kosuke@jaea.go.jp (K. Tanaka).

0022-3115/$ - see front matter
doi:10.1016/j.jnucmat.2006.05.052

In this study, the fuel rod performance was investigated for the fuel assembly which was irradiated to the highest burnup. The focus was placed on elucidating the corrosion behavior of the cladding inner surface which significantly affects fuel rod integrity.

The shape of the fission yield spectrum is slightly different for ^{235}U and ^{239}Pu [3]. A clear difference between these two nuclei is the upward shift of the larger mass peak in the fission of ^{239}Pu. This shift means that the fission yields of non-oxidative metal elements increase in the fission of ^{239}Pu, compared with those of ^{235}U [4]. As a result, the oxygen potential in the MOX fuel rod increases with the increase of burnup. It is, thus, expected that cladding surface is corroded more easily in MOX fuel rods than in UO_2 fuel rods. The results obtained in this study were compared from this viewpoint with those reported in UO_2 fuel rods.

2. Experimental

2.1. Specimens

The fuel assembly, E09, used in this study consisted of 36 fuel rods, bundled concentrically in three layers of inner, intermediate, and outer rings. Fig. 1 shows drawings of the fuel assembly and fuel rod [2]. The fuel pellets were fabricated from a mixture of UO_2 powder and $50\%UO_2$–$50\%PuO_2$ powder obtained by ball milling. UO_2 powder were prepared by the ADU (ammonia di-uranate) method and $50\%UO_2$–$50\%PuO_2$ powder were obtained by the MH (direct de-nitration of uranyl nitrate and plutonium nitrate by microwave heating) method [5]. Thus, the homogeneity of plutonium was good in the pellets.

Table 1 lists specifications of the E09 fuel. In order to make the neutron distribution in the fuel assembly as homogeneous as possible, the fissile content in the fuel pellets decreases stepwise toward the outer ring in the radial direction and along the axial direction. The fuel pellets (95% TD) were 12.4 mm in diameter and 13 mm in height. Two materials were used for the cladding tube; one was standard Zircaloy-2 (Zry-2) and the other was Zry-2 with zirconium liner covered on the inner surface of the cladding tube.

2.2. Irradiation history

As shown in Fig. 2, the E09 fuel assembly was loaded and irradiated at the central position in the

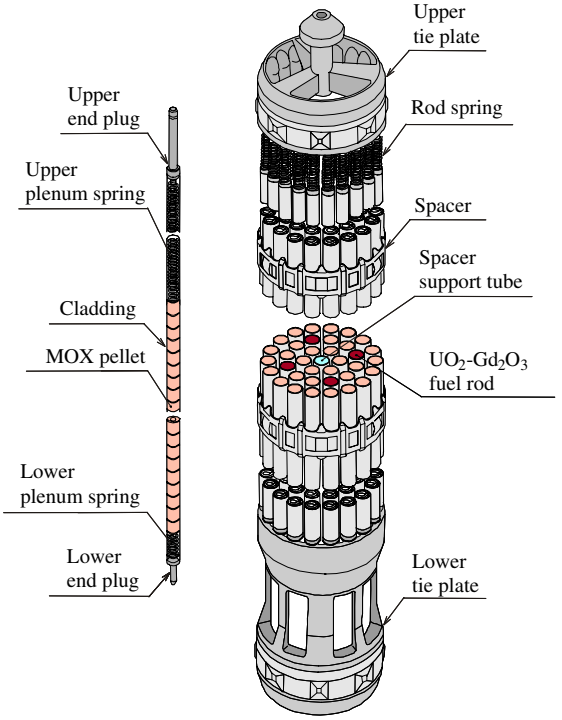

Fig. 1. Configuration of FUGEN E09 fuel assembly.

Table 1
Specifications of FUGEN E09 fuel

MOX fuel pellet		
	Fissile content[a]	2.6–5.0%
	Diameter	12.4 mm
	Height	13 mm
	Density	95% TD
Fuel rod cladding		
	Material	Zry-2 and Zry-2+Zr liner (thickness: 0.07 mm)
	Outer diameter	14.5 mm
	Inner diameter	12.7 mm
	Wall thickness	0.9 mm
Fuel rod		
	Length	4061 mm
	Fuel active length	3640 mm
	Plenum length: upper/lower	357 mm/30 mm
	Filling gas and pressure	He: 0.3 MPa

[a] $(^{239}Pu + ^{241}Pu + ^{235}U)/(Pu + U)$.

FUGEN core for 10 operation cycles. Fig. 3 shows the history of peak powers in the three fuel regions in this assembly. The maximum linear heat ratings for the entire irradiation period were 25.1 (inner), 34.1 (intermediate) and 43.2 (outer) kW/m. The

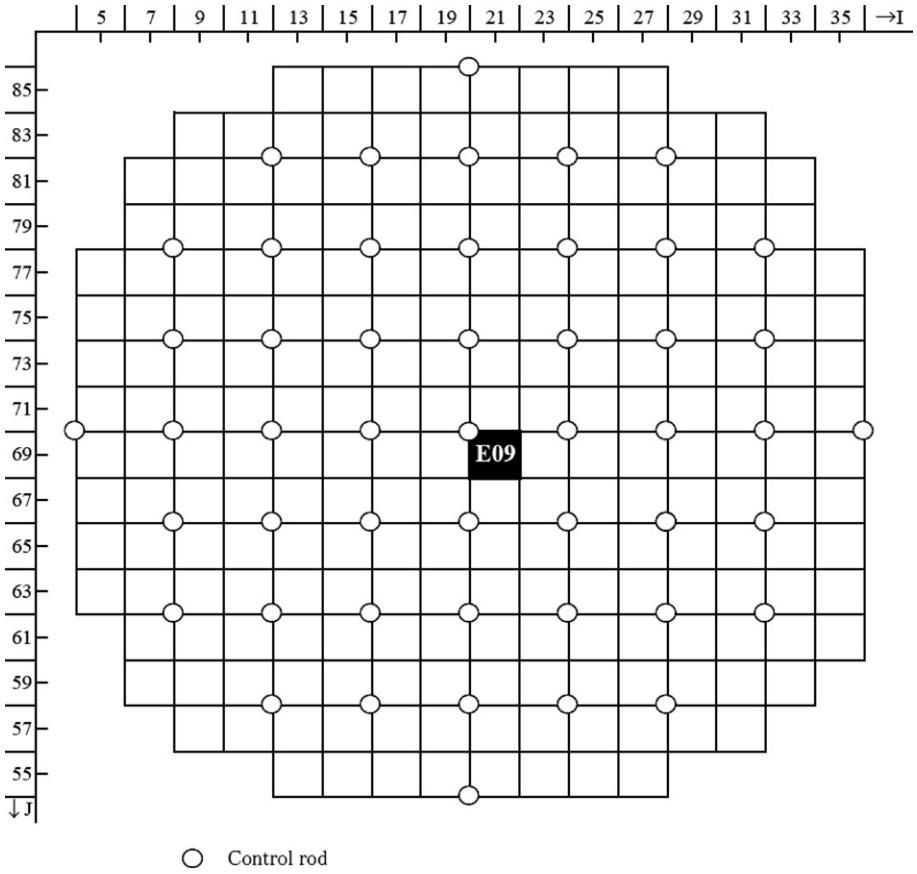

Fig. 2. Schematic illustration of irradiation position for E09 in FUGEN core.

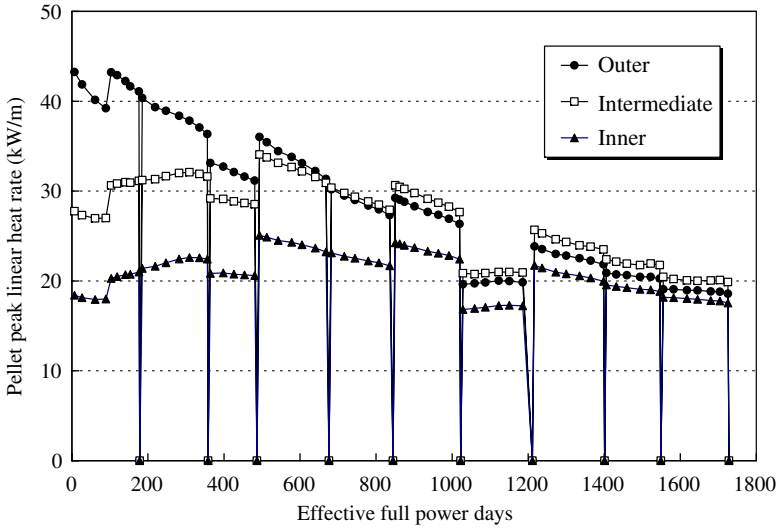

Fig. 3. The history of peak power in each fuel region in E09 MOX fuel assembly.

irradiation lasted about 1725 EFPD (effective full power days) and reached the maximum burnups of 34.9 (inner), 45.0 (intermediate) and 47.5 (outer) GWd/t.

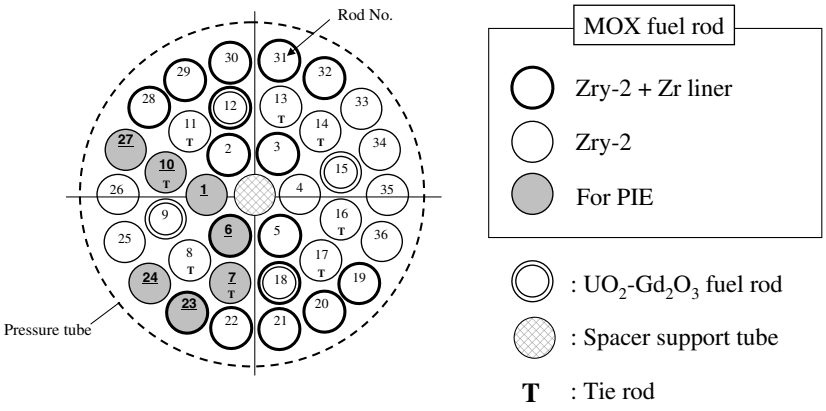

Fig. 4. Top view drawing of fuel rods in FUGEN E09 fuel assembly.

2.3. Fuel rods and specimens for post irradiation examinations

Fig. 4 shows a schematic layout of 36 fuel rods in E09 fuel assembly. Four fuel rods contained UO_2–Gd_2O_3 pellets as a burnable poison. Fuel pellets in the other rods were MOX fuel. In addition, Zry-2 claddings were utilized in 20 fuel rods and Zry-2 claddings lined with Zr metal were used in 16 fuel rods. Seven fuel rods (two inner, two intermediate and three outer ring rods) which are shaded in Fig. 4 were subjected to the post irradiation examination.

Two types of specimens were cut from the seven fuel rods; one was the cross-sectional specimen to examine the microstructure on the cross section of a fuel rod, in which thickness of the reaction zone was measured and existence of the bonding layer was checked. The other was the longitudinal specimen to observe morphology of the cladding inner surface along a longitudinal section after removing the fuel pellets. Detailed characteristics of the examined fuel rods are summarized in Table 2.

2.4. Preparation of specimens and post irradiation examinations

Fuel rods were cut into some segments of about 20 mm in length. Longitudinal specimens were prepared by axially cutting a segment into two parts and mechanically removing the fuel pellets from the cladding. Cut specimens were ultrasonically cleaned in a xylene bath.

Cross-sectional specimens were prepared by the following processes; a segment (about 20 mm in length) was impregnated with epoxy resin in vacuum and cut transversely into discs of about 5 mm in thickness while using kerosene as lubricant. These disks were mounted into holders using epoxy resin, and then were ground and mirror-polished with anhydrous lubricant.

The cross-sectional specimens were mainly examined with an optical microscope. Some specimens were also examined by a scanning electron microscope (SEM) and an electron probe micro-analyzer (EPMA).

The macrostructures of inner surfaces on the longitudinal specimens were observed by a kind of telescope. In addition, some of these specimens were also sectioned into small pieces and subjected to secondary electron imaging and element distribution measurements by EPMA.

3. Results

3.1. Microstructure

Fig. 5(a) shows a typical microstructure on a cross section of fuel rod O-24 which was irradiated to 47 GWd/t in the outer ring of the assembly. Some cracks were observed along the radial and circumferential directions of the fuel pellet. These crack patterns were not so different from those seen in conventional UO_2 fuel. No remarkable change in diameter or distinct decrease in thickness was seen in the cladding. Fig. 5(b) is an enlarged view of the microstructure of the fuel-cladding gap region. The re-crystallized structure known as rim structure was observed at the fuel pellet periphery and a slight amount of the reaction layer appeared on the inner surface of the cladding.

Fig. 6 shows a secondary electron image (SEI) and characteristic X-ray images of U, Pu, Zr, O

Table 2
Characteristics of specimens

	Fuel rod	Rod No.	Specimen No.	Pu content (wt%)	DFRT[a] (mm)	Max. LHR (kW/m)	Burnup (GWd/t)	Cladding material
Cross section	Inner ring	I-1	0101-MMi	5.62	745	18.2	26.2	Zry-2
			0201-MN	4.77	2971	23.0	32.4	
			0301-MS	4.77	3160	21.7	31.1	
			5001-MH	4.77	1330	24.3	34.4	
	Intermediate ring	M-7	0607-MMi	5.66	855	28.1	39.2	Zry-2
			0807-MH	4.77	1565	33.9	45.0	
			0907-MH	4.77	2625	33.4	43.7	
			1007-MS	4.77	2805	32.8	43.3	
			5107-MH	4.77	1330	33.0	44.3	
			5207-MMi	5.62	3320	28.8	39.8	
		M-10	5310-MH	4.77	1330	33.0	44.3	Zry-2
			5410-MMi	5.62	3325	28.7	39.8	
	Outer ring	O-23	1923-MH	2.59	1565	42.7	47.5	Zry-2 + Zr liner
			5523-MH	2.59	1330	39.9	47.0	
			5623-MMi	3.01	3320	42.3	41.7	
		O-24	2424-MH	2.62	1565	42.7	47.5	Zry-2
			2624-MH	2.62	2595	42.7	46.0	
			5724-MH	2.62	1330	39.9	47.0	
			5824-MMi	3.01	3320	42.3	41.7	
		O-27	2827-MH	2.62	1545	42.5	47.5	Zry-2
Cladding inner surface	Inner ring	I-6	8306-CH	4.77	1631	25.1	34.9	Zry-2 + Zr liner
	Intermediate ring	M-10	8510-CH	4.77	1350	33.1	44.5	Zry-2
	Outer ring	O-23	8623-CH	2.59	1350	40.3	47.1	Zry-2 + Zr liner

[a] Distance from rod top.

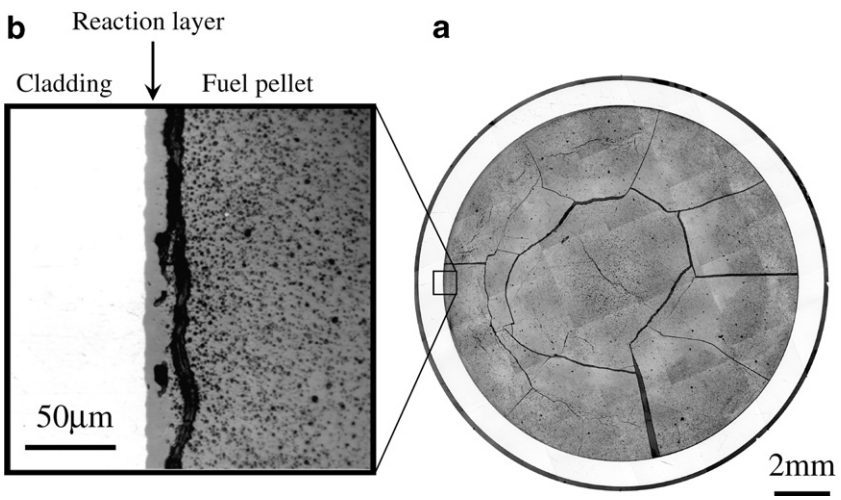

Fig. 5. Oxide layer on the cladding inner surface.

and Cs around the fuel-cladding gap adjacent to the region shown in Fig. 5(b). The gap, in which a small amount of fuel was adhered to the cladding surface, evolved along the corrugated surface of reaction

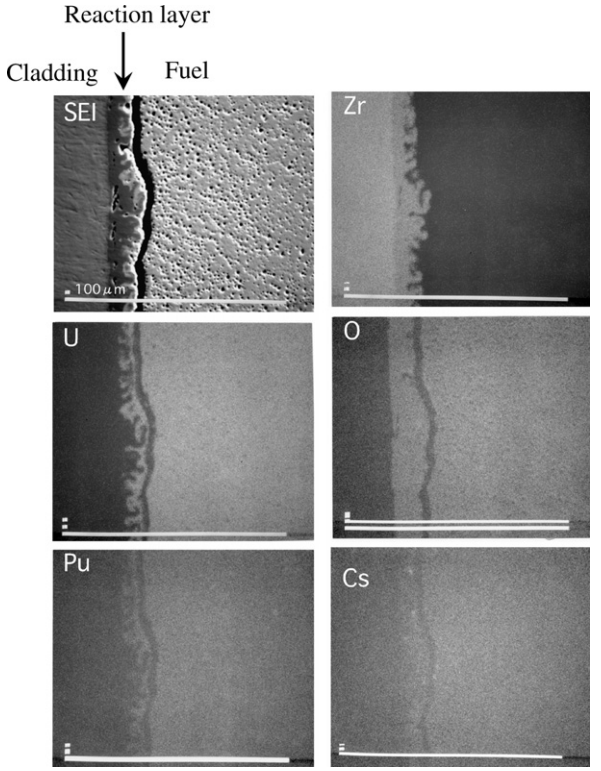

Fig. 6. Secondary electron image and characteristic X-ray images around fuel-cladding gap.

zone on the cladding inner surface in the outermost region of the fuel pellet. It was most likely that this gap opened while cooling when the reactor was shutdown. That is, the gap was closed during irradiation, but it opened due to the difference of volume change between the fuel and cladding during the shutdown. At this time, the small amount of fuel was adhered to the cladding by formation of the bonding layer between the cladding and fuel.

In order to examine more detailed distributions of elements in the region near the gap, radial line scans of EPMA were done from the cladding to the fuel pellet matrix. Fig. 7 shows typical EPMA radial scan results. The reaction layer consisted of two types of layers; one was a compound formed of the main cladding elements, Zr and oxygen (oxide layer), and the other was formed of Zr, fuel elements and fission products (bonding layer). In the bonding layer, the amount of Zr decreased and U, Pu and Cs contents increased on approaching the gap.

The bonding layer described above could be observed in the fuel rods taken from the outer and intermediate rings of the fuel assembly, which were irradiated to high burnup a little over 40 GWd/t, but it was not observed in the fuel rod irradiated to the burnup below 35 GWd/t in the inner ring. To investigate the influence of the Pu spot on the fuel-cladding chemical interaction FCCI, microstructures were observed in the same fuel rod in regions with and without a Pu spot. Fig. 8 shows the SEI of a Pu spot of about 10 μm diameter located at the outermost region of the fuel pellet. No distinct difference could be seen between thicknesses of reaction layers on the cladding inner surfaces adjacent to the fuel regions with and without the Pu spot. No Pu spot larger than 10 μm could not be observed in this study, and it was, thus,

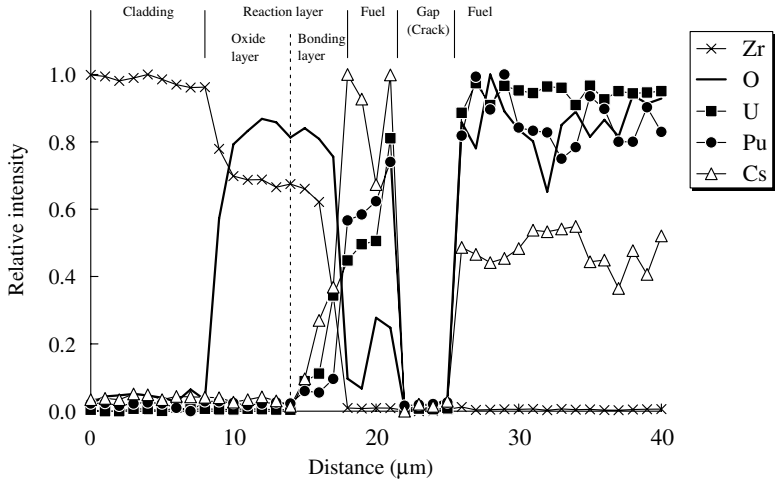

Fig. 7. Distributions of Zr, U, Pu, O and Cs in the region near the fuel-cladding gap.

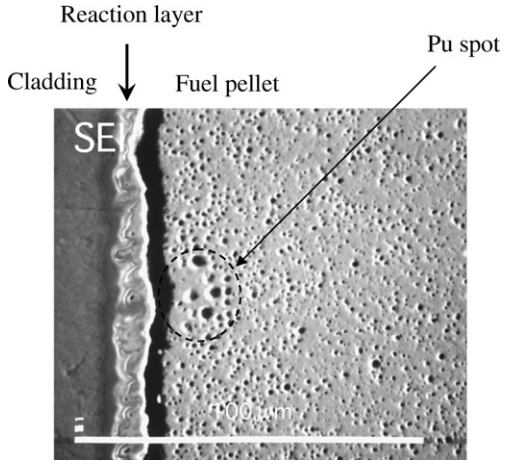

Fig. 8. Secondary electron image of cladding inner reaction layer around the Pu spot located at the pellet outer surface.

concluded that the 10 μm Pu spot had no effect on the FCCI.

3.2. Burnup dependence of reaction layer thickness

Fig. 9 shows the relationship between pellet average burnup and maximum thickness of reaction layer on the cladding inner surface. The thickness was measured on optical micrographs of the cladding inner surface. This thickness was the sum of both oxide and bonding layer thicknesses, because it was difficult to define the boundary between them on the optical micrograph. In this measurement, however, the layer which was clearly identified as adhered fuel pieces was not included in the thickness measurement.

In Fig. 9 the reaction layer thickness on the cladding inner surface increased with increased burnup and reached about 12 μm at the maximum burnup of 47 GWd/t. There was also no distinct difference between the reaction layer thicknesses on the inner surfaces of claddings with and without the Zr inner liner. This result was in good agreement with the one previously reported on UO_2 fuel cladding by Asahi et al. [6].

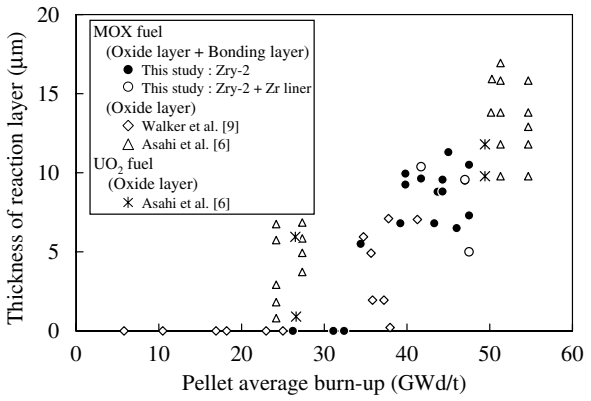

Fig. 9. Thickness of oxide layer on the cladding inner surface as a function of pellet average burn-up.

3.3. Structural morphology and elemental distribution on the cladding inner surface

Fig. 10 shows a typical macroscopic structure on the cladding inner surface of specimen 8623-CH observed by the telescope. The deposit morphologies were of three types: (a) sharply defined liner stripes of tiny nodular deposits, which were located in the cladding inner surface facing the cracks in the fuel pellet; (b) more massive deposits located at pellet-pellet interfaces; and (c) circular stratified deposits or mound-like deposits located randomly.

Fig. 11 shows the SEI and characteristic X-ray images of elements taken on the cladding inner surface of specimen 8623-CH. The Zr spot was little observed in the region rich in fuel constituents. On the other hand, the concentrations of fission products, Cs, Ba, Te, I were high in the region where the fuel constituents were lacking. Oxygen, which is related to the reaction zone and fuel, was uniformly distributed over the whole cladding inner surface. The Ag and Cd spots were sparsely found throughout the whole cladding inner surface region. The morphology and elemental distributions described above were not so different from those in BWR UO_2 fuel rods irradiated to high burnup, from which the fission gas release rate is high [7,8].

4. Discussion

4.1. Reaction layer thickness on the cladding inner surface

Comparison of the fission spectra of ^{235}U and ^{239}Pu shows that the fission yield curve of ^{239}Pu shifts to the higher mass side which results in the larger yield of non-oxidizable elements. It is, thus, expected that the reaction layer thickness is larger in MOX fuel rods than in UO_2 rods due to the difference in the increase of oxygen potentials in them, if the initial O/Ms ratio are same in both fuels.

Some papers [6,9,10] have reported on the reaction layer thickness of in irradiated MOX fuel rods for LWRs. Asahi et al. [6] and Walker et al. [9] investi-

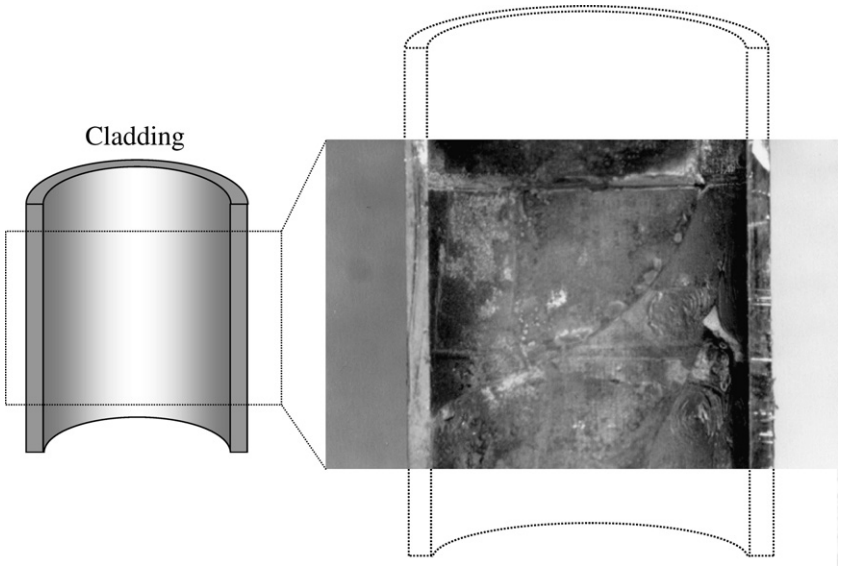

Fig. 10. Deposits on the cladding inner surface.

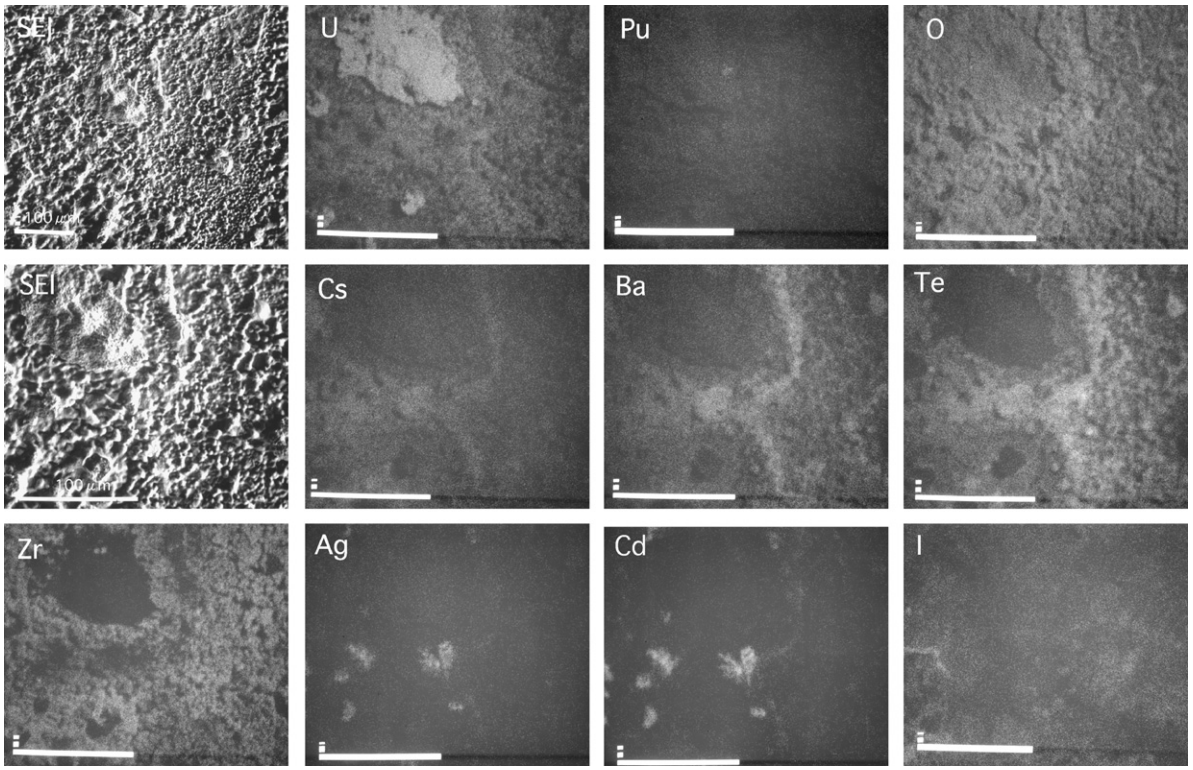

Fig. 11. Secondary electron images and characteristic X-ray images of the deposits on the cladding inner surface.

gated the dependence of thickness on the burnup. The former study clarified that the thickness increased with the burnup and was smaller than 20 μm even at 55 GWd/t. The latter study showed that no reaction took place below 35 GWd/t, but the reaction layer thickness was 1–7 μm at 40 GWd/t.

In addition, Deramaix et al. [10] studied the oxidation behavior of the cladding inner surface in

MOX fuel rods and found that the reaction layer thickness was below 14 μm until 50 GWd/t. In three studies described above, it was seen that the thickness of the oxidation (reaction) layer was similar in both MOX and UO_2 fuel rods. In the present study, the initial O/M ratio of MOX fuel was in the range 1.98–1.99, and the reaction layer thicknesses were smaller than 15 μm, and their burnup dependence was similar to that of UO_2 fuel, as shown in Fig. 9. According to Adamson's evaluation[11], the O/M increase per 10 GWd/t due to the increase of extra free oxygen in MOX fuel during irradiation is in the range 0.002–0.004. Then, this extra oxygen is expected to be expired only in the increase of O/M ratio in the fuel without cladding oxidation until 30–40 GWd/t. After then, this extra oxygen in MOX fuel begins to contribute to the cladding oxidation, but considerable difference between UO_2 and MOX fuels seem to appear beyond ~60 GWd/t. It is, therefore, concluded that the reaction layer thicknesses are similar in both UO_2 and MOX fuel rods under the range of 50 GWd/t.

Some methods have been developed to fabricate MOX fuel. The fuel pellets were fabricated by MIMAS in the studies of Asahi et al. [6] and Deramaix et al. [10], and by both OCOM and AuU/PuC routes in the study of Walker et al [9]. In addition, the MH method was applied to the fabrications of fuel in this study and that of Asahi et al. [6]. Slight differences in the fuel microstructure, such as grain size, presence and density of Pu spots, have been observed, depending on the fabrication method, but no distinct difference could be found in the reaction layer thicknesses among all the studies described above. It can be, therefore, concluded that the fabrication method does not affect the reaction layer thickness on the cladding inner surface.

Local burnup is larger in the Pu spot region than in other fuel regions. It is expected from the reason described above that the oxidation reaction is facilitated at the cladding inner surface adjacent to Pu spots. Walker et al. [9] have reported that the oxidation layer was two times thicker on cladding inner surface around the Pu agglomerates than on the other cladding inner surface. As seen in Fig. 8 , however, the plutonium spot adjacent to cladding gives no significant effect on the thickness of reaction layer in this study. This result is most likely due to the good homogeneity, that is, small size of plutonium spot of MOX fuel examined in this study had little effect on the oxidation on the cladding surface.

4.2. Formation of bonding layer

The formation of bonding layer is an important phenomenon as the mechanical interaction between fuel pellet and cladding for highly burnt fuels. The bonding layer limits the independent movements of fuel pellet and cladding, and thus generates higher stress on the cladding during transient reactor operation. Nerman [12] analyzed the fuel-cladding interaction during transient reactor operation by an FEM code, and has reported that the bonding leads to higher stress on the cladding inner surface as compared to the friction conditions.

Une et al. [13] and Nogita et al. [14,15] carried out systematic studies on bonding layer formation in both PWR and BWR fuel rods, and have clarified the formation mechanism. In addition, they calculated the linear heat rating necessary to establish strong contact between the fuel and cladding from the data on the residual gap versus burnup previously reported in LWR fuel rods, using a pellet thermal deformation model, and their results have been expressed as functions of linear heat rating and burnup.

Table 3 shows the comparisons of initial fuel-cladding gap, internal pressure and coolant pressure between ATR and BWR fuel rods. As indicated in this table, the initial fuel-cladding gap is larger in ATR fuel than in BWR one. However, the initial pressure difference between the inside and outside surfaces of ATR fuel rod cladding is almost same as BWR one. Figs. 12 and 13 [16] show the outer diameter of cladding and fuel swelling as a function of burn-up in ATR fuel rods. From these figures, the outer diameter of cladding is minimum around 30 GWd/t and thereafter increases with increasing burnup, leading to a strong contact between fuel and oxidized cladding surface, just likely in the case of BWR fuel rod. Fig. 14 compares the present data with data of Une et al. in the region of burnup below 50 GWd/t. The threshold value of about

Table 3
The comparisons of initial fuel-cladding gap, internal pressure and coolant pressure

Fuel rod	Initial fuel – cladding gap (mm)	Internal pressure (MPa)	Coolant pressure (MPa)
ATR–MOX (This study)	0.3	0.3	6.7
BWR–MOX, BWR–UO_2 [6]	0.2	0.5	7.0

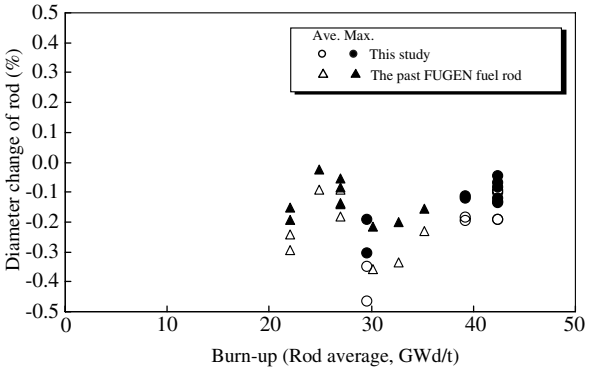

Fig. 12. Burn-up dependence of ATR fuel rod cladding diameter change.

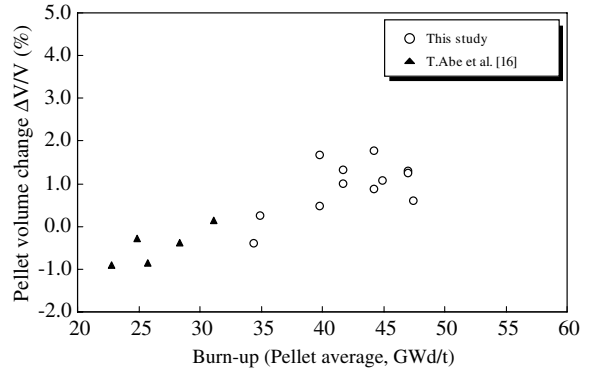

Fig. 13. Burn-up dependence of ATR–MOX pellet diameter change.

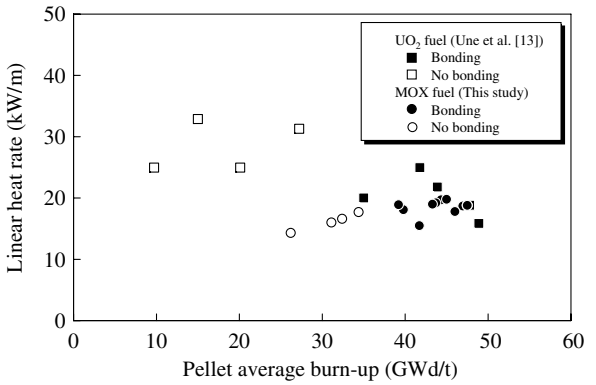

Fig. 14. Bonding formation in MOX fuel rods in correlation with pellet average burn-up and linear heat rate.

35 GWd/t to establish partial bonding is found in both studies. It is, thus, suggested that the formation behavior of the bonding layer is similar in both BWR UO_2 and ATR MOX fuel rods.

5. Conclusion

The cladding inner surface corrosion and its resulting fuel-cladding bonding were investigated in the ATR MOX fuel rods irradiated to 34.9, 45.0 and 47.5 GWd/t, by using a telescope, optical microscope, SEM and EPMA.

The reaction layer was observed in specimens with burnups higher than about 35 GWd/t. and the relationship between the reaction layer thickness and burnup was similar to that reported already. The reaction layer consisted of two types of layers. The first layer adjacent to the cladding was mainly comprised of a compound of the main cladding constituents Zr and oxygen, while the main components of the second layer near the gap, which was probably formed during cooling when the reactor was shutdown, were U, Pu, fission products and oxygen.

Whether or not the bonding layer evolved between the fuel and cladding was discussed from the dependence of cladding outer diameters and fuel swelling on the burnup. Then, the presence or absence of bonding was evaluated as functions of burnup and linear heat rating. It was found that the bonding appeared above the burnup of 35 GWd/t and the linear heat rating of about 20 kW/m. The results were similar to those of Une et al. [13].

Acknowledgements

The authors are grateful to Dr H. Furuya (Emeritus Professor of Kyushu University), for his suggestions and discussions in this study. They also thank Messrs Y. Ohsato, Y. Onuma, and S. Nukaga (Nuclear Technology and Engineering Corporation) for help in the experiments.

References

[1] S. Maeda, H. Nakazawa, T. Abe, Proceedings of the International Conference on Global Environment and Advanced Nuclear Power Plants, GENES4/ANP2003, Kyoto, Japan, Paper 1150 (2003).
[2] T. Ozawa, Y. Ikusawa, T. Abe, K. Maeda, Proceedings of the 2004 International Meeting on LWR Fuel Performance, Orlando, FL, September 19–22, Paper 1031 (2004).
[3] J.H. Davies, F.T. Ewart, J. Nucl. Mater. 41 (1971) 143.
[4] H. Kleykamp, J. Nucl. Mater. 131 (1985) 221.
[5] M. Koizumi, K. Ohtsuka, H. Isagawa, H. Akiyama, A. Todokoro, Nucl. Technol. 61 (1983) 55.
[6] K. Asahi, M. Oguma, T. Matsumoto, T. Toyoda, Proceedings of the 1994 International Topical Meeting on Light Water Reactor Fuel Performance, West Palm Beach, FL, April 17–21 (1994) 726.

[7] A. Ohuchi, T. Nomata, S. Koizumi, T. Aoki, IAEA Specialists' Meeting on Post Irradiation Examination and Experience, Tokyo, Japan, November 26–30 (1984) JA-8.
[8] A. Ohuchi, H. Sakurai, Proceedings of ANS Topical Meeting on LWR Fuel Performance, Williamsburg, VA, April (1988) 180.
[9] C.T. Walker, W. Goll, T. Matsumura, J. Nucl. Mater. 245 (1997) 169.
[10] P. Deramaix, D. Haas, J. Van de Velde, Nucl. Technol. 102 (1993) 47.
[11] M.G. Adamson, E.A. Aitken, S.K. Evans, W.H. McCarthy, GEAP-14075 (1976).
[12] H. Nerman, Nucl. Eng. Des. 56 (1980) 289.
[13] K. Une, K. Nogita, S. Kashibe, T. Toyonaga, M. Amaya, Proceedings of the 1997 International Topical Meeting on LWR Fuel Performance, Portland, OR, March 2–6 (1997) 478.
[14] K. Nogita, K. Une, J. Nucl. Sci. Technol. 34 (1997) 679.
[15] K. Nogita, K. Une, IAEA-TECDOC-1036 (1998) 377.
[16] T. Abe, S. Maeda, H. Nakazawa, Proceedings of 13th International Conference on Nuclear Engineering, Beijing, China, May 16–20 (2005) No. 50298.